12-1999

Stellar Angular Diameters of Late-Type Giants and Supergiants Measured with the Navy Prototype Optical Interferometer

Tyler E. Nordgren
U.S. Naval Observatory, Flagstaff, AZ

M. E. Germain
U.S. Naval Observatory, Flagstaff, AZ

J. A. Benson
U.S. Naval Observatory, Flagstaff, AZ

D. Mozurkewich
Naval Research Laboratory, Washington, D.C.

Jeffrey J. Sudol
West Chester University of Pennsylvania, jsudol@wcupa.edu

See next page for additional authors

THE ASTRONOMICAL JOURNAL, 118:3032–3038, 1999 December

STELLAR ANGULAR DIAMETERS OF LATE-TYPE GIANTS AND SUPERGIANTS MEASURED WITH THE NAVY PROTOTYPE OPTICAL INTERFEROMETER

TYLER E. NORDGREN,[1] M. E. GERMAIN,[1] J. A. BENSON,[1] D. MOZURKEWICH,[2] J. J. SUDOL,[3,4] N. M. ELIAS II,[1] ARSEN R. HAJIAN,[5] N. M. WHITE,[6] D. J. HUTTER,[5] K. J. JOHNSTON,[5] F. S. GAUSS,[5] J. T. ARMSTRONG,[2] T. A. PAULS,[2] AND L. J RICKARD[2]

Received 1998 September 4; accepted 1999 August 18

ABSTRACT

We have measured the angular diameters of 50 F, G, K, and M giant and supergiant stars using the Navy Prototype Optical Interferometer at wavelengths between 649 and 850 nm and using three baselines with lengths up to 37.5 m. Uniform-disk diameters, obtained from fits to the visibility amplitude, were transformed to limb-darkened diameters through the use of limb-darkening coefficients for plane-parallel stellar atmosphere models. These limb-darkened diameters are compared with those measured with the Mark III optical interferometer and with those computed by the infrared flux method. Sources of random and systematic error in the observations are discussed.

Key words: stars: fundamental parameters — techniques: interferometric

1. INTRODUCTION

The Navy Prototype Optical Interferometer (NPOI) has been in routine operation with three baselines since 1996, and its operation has recently been described by Armstrong et al. (1998). Scientific projects undertaken to date include modeling of binary star systems of small angular separation (Benson et al. 1997; Hummel et al. 1998) and the determination of limb darkening in the atmospheres of late-type luminous stars (Hajian et al. 1998). Beginning in the fall of 1997, we initiated a program to measure the angular diameters, θ, of a large sample of luminous stars, most of which have $\theta \leq 3$ mas. With the limited u-v plane coverage available with the present baseline geometry, we are not able to measure detailed stellar morphology (i.e., oblateness) or surface structure. Completion of the full complement of six siderostats, and extension of the baselines to 437 m, will result in better u-v coverage and increased diameter precision.

Here we report uniform-disk diameters, obtained from fits to the visibility amplitude. They are transformed to limb-darkened diameters through the use of brightness distributions computed from model atmospheres. We also assess random and systematic errors and compare our diameters with those obtained with the Mark III (Mozurkewich et al. 1999) and from the infrared flux method (Bell & Gustafsson 1989; Blackwell & Lynas-Gray 1994). Our stars are restricted to declinations available to the NPOI, north of declination $-20°$, but otherwise distributed uniformly around the sky. Sources were chosen with expected diameters that can be measured best with our longest baseline, oriented east-west with a length of 37.5 m. We also restricted our wavelength coverage to the 10 reddest spectral channels, ranging from 649 to 850 nm, where the optical throughput of the instrument is highest. The mean wavelength is 740 nm. Generally, we selected stars with expected angular diameters less than ~ 5 mas, so that all the spatial frequencies sampled are within the first null of the visibility function. Given the current baseline lengths, combined with the expected NPOI calibration and observational errors, a lower limit of ~ 1.5 mas was chosen. Finally, based upon the current ability to track fringes, the source list was restricted to stars with magnitude $m_I \leq 3.5$.

These selection criteria result in about 400 stars of luminosity class IV or brighter that span the range of spectral types from A to early M. Most of the stars are normal giants of luminosity class III. The criteria allow us to examine sources that have not yet been systematically measured by other interferometers in the optical part of the spectrum. Recent work on stars of comparable angular size has, however, been done at longer wavelengths using the Palomar Testbed Interferometer (PTI; van Belle et al. 1999). To date, 50 stars in our sample have been observed with the NPOI. In this paper we report the observations of these stars with a discussion of their mean diameters and sources of error.

2. OBSERVATIONS AND DATA REDUCTION

Afocal 12.5 cm beams of light are fed through vacuum pipes from three astrometric siderostats (center, east, and west) into beam compressors that reduce the beams to a diameter of 3.5 cm. These beams continue into fast delay lines for path-length compensation and then onto the beam-combiner table. After combination, the center-east, east-west, and west-center pairs are passed through separate prisms and onto 32-element avalanche photodiode detector arrays. The dispersion gives a roughly constant spectral interval of about 40 nm^{-1}. We use spectral channels centered approximately at 649, 665, 683, 702, 723, 744, 768, 794, 821, and 849 nm for the observations reported in this paper. The bluer channels were eliminated because of their low signal-to-noise ratio for the stars observed.

Calibration sources were chosen from a list of stars estimated to have angular diameters ≤ 1 mas as computed

[1] Astrometry Department, US Naval Observatory, NPOI, P.O. Box 1149, Flagstaff, AZ 86002-1149.
[2] Remote Sensing Division, Naval Research Laboratory, Code 7210, Washington, DC 20375.
[3] Department of Physics and Astronomy, University of Wyoming, Box 3905, University Station, Laramie, WY 82076.
[4] NASA PASS Grant Fellow, University of Wyoming.
[5] Astrometry Department, US Naval Observatory, 3450 Massachusetts Avenue, NW, Washington, DC 20392.
[6] Lowell Observatory, 1400 West Mars Hill Road, Flagstaff, AZ 86001.

from their observed colors and magnitudes (Mozurkewich et al. 1991). Measured with the full 37.5 m baseline, a 1 mas diameter star yields a visibility amplitude squared (V^2) of 0.86, for a perfect interferometer. V^2 on the two shorter baselines is higher. Calibrators were picked so that they were observed close in time and space to the science targets, thereby minimizing the effects of atmospheric variation and instrumental response. The calibrators and their estimated diameters are listed in Table 1. Fringe data were sampled at 500 Hz. For a 90 s scan the sampling typically results in 45,000 independent samples of V^2 in each of the 10 spectral channels. The samples at each wavelength in each 90 s scan were averaged to form a single value of V^2; the averaging process yields V^2 at 10 different spatial frequency points, one for each wavelength. Details of the V^2 calculation from the raw data, including removal of noise bias, may be found in Armstrong et al. (1998) and Hummel et al. (1998).

The standard procedure was to observe a calibrator immediately before or after a science source. Raw squared visibilities for each scan were calculated using standard algorithms in the NPOI software pipeline (Armstrong et al. 1998; Hummel et al. 1998; Hajian et al. 1998). For each calibrator scan, the visibilities were corrected for the partial resolution of the interferometer to yield the instrumental V^2. The average V^2 of each science source was then divided by the instrumental V^2 scan obtained immediately before or after the science-source scan, whichever was taken closest in time. The resulting ratio yields the calibrated V^2 versus wavelength for the science source.

3. UNIFORM-DISK DIAMETERS

For each scan we fitted a simple uniform disk function to the calibrated visibilities:

$$V^2 = \left[\frac{2J_1(\pi\theta_u v)}{\pi\theta_u v}\right]^2, \quad (1)$$

where J_1 is the first-order Bessel function of the first kind, θ_u is the uniform-disk diameter, and v is the spatial frequency. For those stars small enough that the observed spatial frequencies did not extend to the first null in the visibility function, only visibilities from the longest baseline (east-west) were used in the diameter fit. For larger stars where all three baselines produced V^2 much less than 1, all baselines were used to determine a diameter.

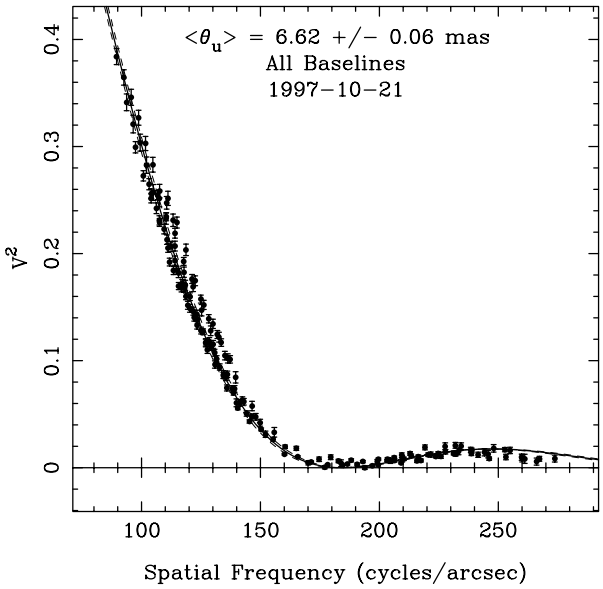

FIG. 1.—Plot of calibrated V^2 vs. spatial frequency for seven scans of γ Aql shown with a simple uniform disk fitted to the data. The best fit to the data (*solid line*) is $\langle\theta_u\rangle = 6.62 \pm 0.06$ mas (with the dashed lines representing the error of the mean).

The error of the fit for each scan was determined from the scatter of the 10 V^2 points about the best-fit function. In this way, we produced a uniform-disk angular diameter and error for each 90 s scan. Whenever possible, we obtained more than one scan of a target and made observations on more than one night to assess the repeatability of the measurements. When multiple scans were obtained on one or more nights, we determined the mean, $\langle\theta_u\rangle$, and standard deviation of the scan diameters for each star. Dividing the standard deviation of the scan diameters by the root of the number of scans we determined the error of the mean, $\sigma_{\langle\theta\rangle}$.

We show two examples of the calibrated visibility data in Figures 1 and 2. In Figure 1, we show a plot of V^2 versus spatial frequency for γ Aql on the night of 1997 October 21. The solid line corresponds to $\langle\theta_u\rangle = 6.62 \pm 0.06$ mas, which is the mean of seven scans observed on this night. This star is one of the larger stars in our program. Figure 2

TABLE 1

CALIBRATION STARS USED

HR No.	Name	θ_{est} (mas)	HR No.	Name	θ_{est} (mas)	HR No.	Name	θ_{est} (mas)
39	γ Peg	0.42	2845.....	β CMi	0.67	7235.....	ζ Aql	0.80
153	ζ Cas	0.26	3975.....	η Leo	0.67	7236.....	λ Aql	0.47
269	μ And	0.69	4033.....	λ UMa	0.62	7420.....	ι^2 Cyg	0.70
542	ϵ Cas	0.43	4368.....	ϕ Leo	0.58	7528.....	δ Cyg	0.79
580	50 Cas	0.50	4554.....	γ UMa	0.92	7750.....	κ Cep	0.30
664	γ Tri	0.50	5107.....	ζ Vir	0.82	7852.....	ϵ Del	0.30
838	41 Ari	0.40	5435.....	γ Boo	1.00	8028.....	ν Cyg	0.52
1122.....	δ Per	0.53	5511.....	109 Vir	0.53	8142.....	σ Cyg	0.70
1165.....	η Tau	0.73	6175.....	ζ Oph	0.84	8454.....	π^2 Peg	0.92
1220.....	ϵ Per	0.43	6396.....	ζ Dra	0.50	8518.....	γ Aqr	0.47
2004.....	κ Ori	0.62	6410.....	δ Her	0.83	8585.....	α Lac	0.50
2540.....	θ Gem	0.78	6789.....	δ UMi	0.40	8634.....	ζ Peg	0.52
2763.....	λ Gem	0.72	7178.....	γ Lyr	0.69			

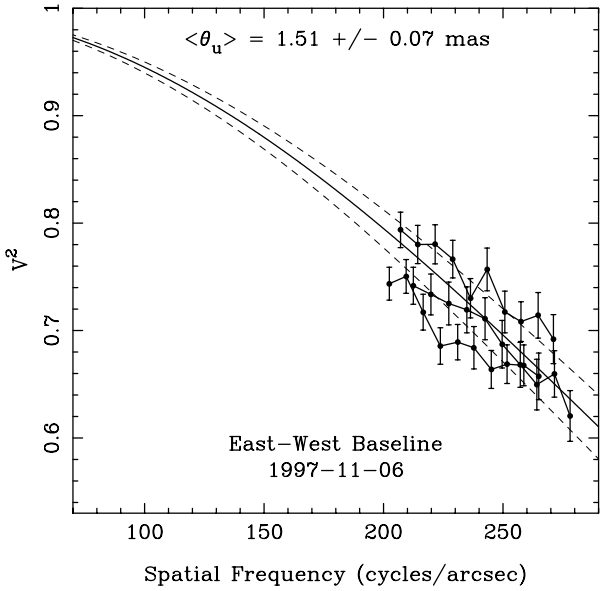

FIG. 2.—Calibrated visibility data for three scans of α Lep. The best fit (*solid line*) to the data is $\langle\theta_u\rangle = 1.51 \pm 0.07$ mas.

shows three scans of α Lep from 1997 November 6, where $\langle\theta_u\rangle = 1.51 \pm 0.07$ mas. Lines connect the 10 spectral channels within each scan. This star is an example of one of the smallest angular diameters observed.

4. SOURCES OF ERROR

The error bars on the squared visibilities shown in Figures 1 and 2 are formal errors based on photon statistics and averaging of the 45,000, 500 Hz samples. Note in Figure 2 that the spread in data points from scan to scan is larger than that indicated by the error bars. If we fit a diameter to a single one of the scans of α Lep in Figure 2, the diameter error estimated from the goodness of fit is almost an order of magnitude smaller than that quoted above. For example, a fit to one scan yields $\theta_u = 1.55 \pm 0.01$ mas. This simply reflects the condition that the scatter in the data is dominated by calibration effects rather than by photon statistics.

Figure 3*a* shows the instrumental squared visibilities (i.e., V^2 has been corrected for the partial resolution of the interferometer, but has not been calibrated) for the science source α Per and its calibrator, δ Per. One can see that in a pairwise calibration scheme, the calibrated V^2 for α Per (the ratio of the two lines) fluctuates. For instance, between 9.0 and 10.5 hours UT, V^2 for the calibrator drops below that of the science source, leading to a higher calibrated V^2 and a smaller measured diameter. Figure 3*b* clearly shows that the measured diameter of α Per drops systematically below the mean during this time.

There are two main phenomena that could cause this observed behavior of the visibilities. The first is systematic differences in the atmosphere between the lines of sight to the calibrator and the science source, which persist for time periods on the order of an hour. Interaction of the surface winds with topography, and the location of the jet stream over the observatory during the course of the night, are just a couple of reasons why the seeing along two different lines of sight, and hence the visibilities of the two sources, could vary differently. Davis & Tango (1996) have shown how the

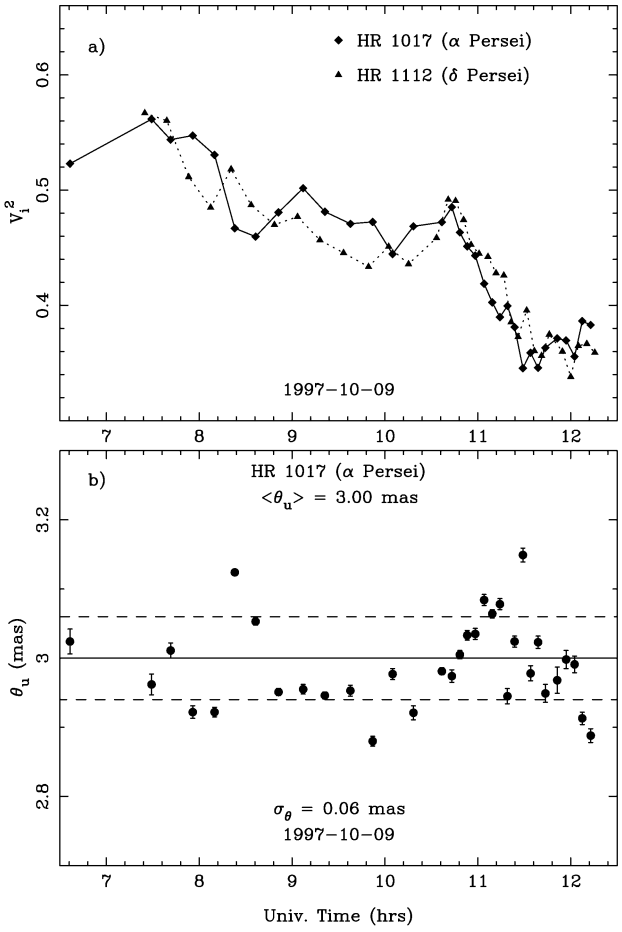

FIG. 3.—(*a*) Uncalibrated V^2 vs. time for the science source α Per and its calibrator, δ Per, where V^2 for both have been corrected for the partial resolution of the instrument. Visibilities are from channel 2 (821 nm) of the longest baseline (east-west). (*b*) Estimated diameter for each scan of α Per, where the error bars are the scatter of V^2 from the 10 spectral channels about the best-fit uniform disk. Note that the error bars are much smaller than the standard deviation shown by the dashed lines (0.06 mas). The mean diameter for the night is the solid line (3.00 mas).

effects of wave-front distortion in the atmosphere over the integration time of the interferometer can be removed from the calculation of V^2. An investigation of this method has begun at the NPOI, which, it is believed, will remove much of the fluctuation seen in Figures 3*a* and 3*b* from future observations. A second phenomenon, unknown systematics in the telescope itself, will not be corrected by this technique.

It is already seen from Figures 3*a* and 3*b* that there are systematic effects on the diameter that have timescales on the order of an hour. It is therefore important to know if there are night-to-night systematics that would prevent the calculation of a well-defined mean diameter. The science source α Per was observed on six nights over the course of a month. To gauge the ability to determine a mean diameter, the individual scans of α Per were divided into nightly bins containing seven scans each. Since different numbers of scans were obtained on each night, some nights possess more than one bin. The mean diameter, $\langle\theta_u\rangle$, for each bin is plotted in Figure 4. The scatter among these mean diameters is found to be 0.030 mas, which may be compared with the scatter of diameters within a single bin divided by $\sqrt{7}$.

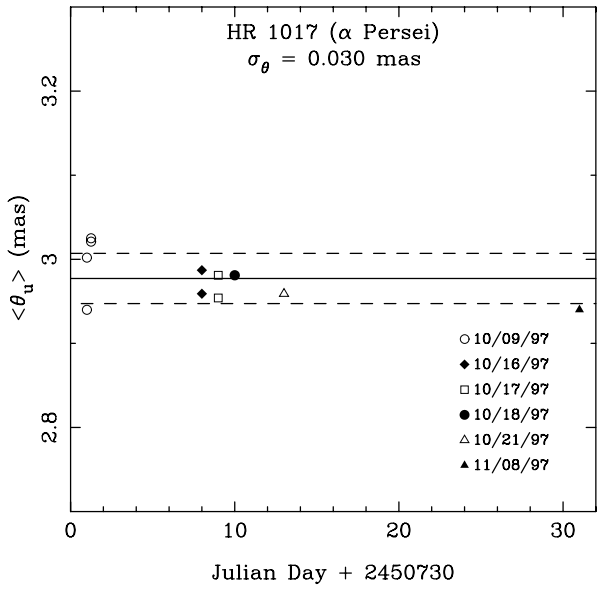

FIG. 4.—Observed $\langle\theta_u\rangle$ for α Per over six nights in the fall of 1997. Each data point is the mean of seven scans. Nights with more than seven scans are represented by multiple data points. The mean of the 11 data points is 2.98 mas, with a standard deviation of 0.03 mas, or 1%.

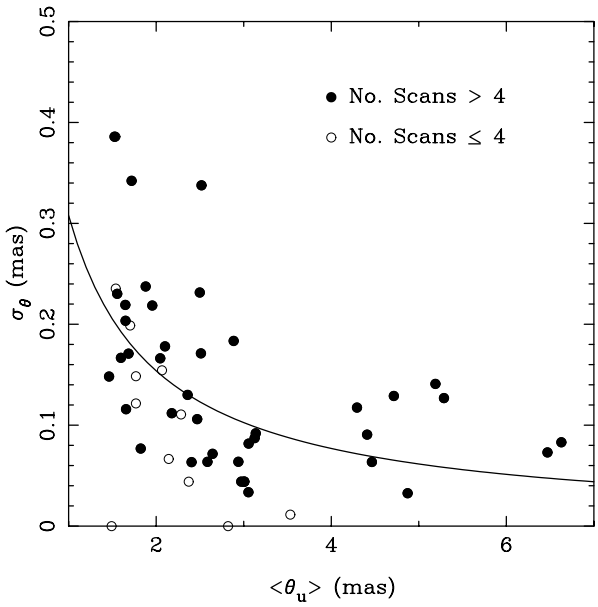

FIG. 5.—Standard deviation of the scan diameters vs. mean diameters for the sample of 50 stars. Open circles represent those stars with fewer than four scans. The solid line is a fit to the data.

The mean of this latter quantity is 0.026 ± 0.011 mas, which is equal, within the uncertainty, to the scatter in the bin means. The equality of these two errors shows that any systematics that affect the diameter measurements take place on timescales that are shorter than the timescale of an hour to several hours, or that are longer than timescales of months. If there were significant systematics with intermediate timescales, they would show up as a larger than expected scatter in the mean diameters of the bins. In particular, there are no large systematics on night-to-night timescales.

One final conclusion to be drawn from Figure 3*b* is that the systematics, whatever the cause, are such that there are correlations between scans taken near in time to one another. When calculating the uncertainty in the mean diameter, then, one should not simply divide the standard deviation of the scan diameters by the square root of the number of scans, as these scans are not necessarily independent. Investigation of the differences between scan diameters as a function of separation in time shows that there is a correlation length of 1.2 hr in the observations. All diameters taken within 1.2 hr of one another are therefore averaged together to produce a single diameter and are counted as a single independent scan. The standard deviation of these independent diameters is then divided by the number of independent scans to produce an error for the mean diameter. Hereafter all mention of "scans" refers to independent scans unless otherwise noted.

For stars with only a few scans, the standard deviation of the scan diameters may not reflect the true scatter of the observations. We therefore use the entire sample of stars having more than four scans to estimate the standard deviation of a single scan diameter, σ_θ, as a function of diameter. Figure 5 shows σ_θ versus the mean diameter for each star in the sample, where the open circles show those stars with fewer than four scans. The solid line is a fit proportional to $1/\langle\theta_u\rangle$ for those stars with more than four scans (*filled circles*), and in all but a few cases the open circles fall below this fit. For those stars with fewer than four scans, the standard deviation in the diameter is replaced by the fit for a star of that diameter.

By following this method, we ensure that we do not underestimate the uncertainty in the final diameter as a result of insufficient data. Once σ_θ is found in this way, the error of the mean diameter ($\sigma_{\langle\theta\rangle}$) is found by dividing by the square root of the number of scans.

In addition to the error represented in the scatter of the individual scan diameters, another error is associated with the uncertainty in the effective wavelength of each channel. For a given visibility predicted by the uniform-disk visibility function, the argument of the Bessel function, which is constant, contains the ratio θ_u/λ. Thus, an error in the wavelength will produce a corresponding error in θ_u. Hajian et al. (1998) adopted an uncertainty equal to half the width of a spectral channel. Subsequent to that work, a Fourier transform spectrometer experiment was used to determine the position of each of the spectral channels. The uncertainty in the channel wavelength was found to be of order 0.3%, as measured from the scatter between the nominal wavelengths and those determined by the experiment. We have computed the diameter error for each star corresponding to a 0.3% relative error and added this in quadrature to $\sigma_{\langle\theta\rangle}$. The dashed lines in Figures 1 and 2 reflect the full quadrature sum of the error of the mean and the error due to wavelength uncertainty.

For simplicity of notation, we define θ_U and σ_U to be the mean uniform-disk diameter and error of the mean (formerly $\langle\theta_u\rangle$ and $\sigma_{\langle\theta\rangle}$). By doing so it is understood that these values, and quantities derived from them, are the averages of multiple observations.

5. LIMB DARKENING

The quantity needed for astrophysical interpretation of the angular diameter is not θ_U, however, but rather the

TABLE 2

DIAMETERS FOR 50 STARS

HR No. (1)	Name (2)	Spectral Type (3)	Ref.[a] (4)	No./Ind. (5)	θ_U (mas) (6)	σ_U (mas) (7)	θ_L (mas) (8)	σ_L (mas) (9)	R ($R_\odot$) (10)	σ_R ($R_\odot$) (11)
21	β Cas	F2 III–IV	M	21/11	2.05	0.05	2.12	0.05	3.80	0.10
163	ϵ And	G6 III	P	10/5	1.68	0.08	1.77	0.08	9.8	0.6
168	α Cas	K0 IIIa	P	12/7	5.29	0.05	5.60	0.06	42.1	1.7
265	υ^2 Cas	G8 IIIb	P	5/4	1.54	0.10	1.63	0.11	11.0	0.8
294	ϵ Psc	G9 III	P	6/5	1.65	0.09	1.74	0.10	10.9	0.8
351	χ Psc	G8.5 III	P	8/5	1.60	0.08	1.69	0.08	24	2
424	α UMi	F7 Ib	B	95/41	3.14	0.02	3.28	0.02	46	3
437	η Psc	G7 IIIa	P	8/5	2.50	0.10	2.64	0.11	26	2
442	χ Cas	G9 IIIb	P	7/6	1.55	0.09	1.64	0.10	11.0	0.8
464	51 And	K3 III	P	3/2	3.53	0.06	3.76	0.07	21.5	0.9
489	ν Psc	K3 IIIa	P	11/8	2.64	0.03	2.81	0.03	34	3
617	α Ari	K2 IIIab	P	45/17	6.47	0.03	6.88	0.04	14.9	0.3
824	39 Ari	K1.5 III	P	6/3	1.77	0.10	1.88	0.11	11.1	0.8
951	δ Ari	K0 III	P	3/2	1.77	0.12	1.87	0.13	10.3	1.0
1017.....	α Per	F5 Ib	M	89/28	2.97	0.01	3.10	0.02	60	7
1256.....	37 Tau	K0 III	P	10/5	1.60	0.08	1.69	0.08	10.1	0.7
1865.....	α Lep	F0 Ib	M	7/4	1.70	0.09	1.77	0.09	74	22
2473.....	ϵ Gem	G8 Ib	P	102/42	4.46	0.02	4.73	0.03	140	35
2973.....	σ Gem	K1 III	B	12/6	2.18	0.05	2.31	0.05	9.3	0.3
3249.....	β Cnc	K4 III	P	57/27	4.71	0.03	5.03	0.04	48	4
3950.....	π Leo	M2 IIIab	P	10/7	4.29	0.05	4.62	0.06	80	10
3980.....	31 Leo	K3.5 IIIb	P	12/6	3.12	0.04	3.33	0.04	30	2
4247.....	46 LMi	K0+ III–IV	P	24/6	2.40	0.03	2.54	0.03	8.2	0.2
4432.....	87 Leo	K3.5 III	P	8/6	3.01	0.02	3.21	0.03	64	12
4518.....	χ UMa	K0.5 IIIb	P	36/8	3.05	0.01	3.23	0.02	20.8	0.8
4932.....	ϵ Vir	G8 IIIab	P	7/6	3.00	0.02	3.17	0.03	10.6	0.3
5200.....	υ Boo	K5.5 III	P	14/6	4.41	0.04	4.72	0.05	38	2
5681.....	δ Boo	G8 III	P	18/9	2.59	0.02	2.74	0.03	10.5	0.2
6220.....	η Her	G7 III	P	4/4	2.29	0.07	2.42	0.07	8.9	0.3
6418.....	π Her	K3 II	P	25/7	4.87	0.02	5.20	0.03	63	4
7176.....	ϵ Aql	K1 III	P	8/5	1.88	0.11	1.99	0.11	10.1	0.7
7314.....	θ Lyr	K0 II	P	14/5	2.10	0.08	2.23	0.09	57	7
7328.....	κ Cyg	G9 III	P	11/7	1.96	0.08	2.07	0.09	8.4	0.4
7525.....	γ Aql	K3 II	P	28/10	6.63	0.03	7.08	0.05	107	11
7570.....	η Aql	F6 Ib–G4 Ib	B	49/25	1.65	0.04	1.73	0.05	66	22
7602.....	β Aql	G8 IV	P	6/3	2.07	0.09	2.18	0.09	3.21	0.14
7796.....	γ Cyg	F8 Ib	B	13/6	2.89	0.07	3.02	0.08	152	36
7957.....	η Cep	K0 IV	P	80/20	2.51	0.04	2.65	0.04	4.08	0.07
8079.....	ξ Cyg	K4.5 Ib–II	P	48/25	5.19	0.03	5.56	0.04	215	40
8252.....	ρ Cyg	G8 III	P	19/13	1.72	0.09	1.82	0.10	7.4	0.4
8414.....	α Aqr	G2 Ib	P	12/5	2.94	0.03	3.08	0.03	77	15
8538.....	β Lac	G9 IIIb	P	116/48	1.82	0.01	1.92	0.02	10.7	0.3
8571.....	δ Cep	F5 Ib–G1 Ib	B	117/46	1.46	0.02	1.52	0.02	51	9
8632.....	11 Lac	K2.5 III	P	9/6	2.47	0.05	2.63	0.05	26.1	1.4
8667.....	λ Peg	G8 IIIa	P	7/2	2.14	0.10	2.26	0.11	29	3
8684.....	μ Peg	G8 III	P	8/3	2.37	0.08	2.50	0.08	9.6	0.4
8923.....	70 Peg	G8 IIIa	P	14/6	1.52	0.16	1.61	0.17	9.4	1.1
8961.....	λ And	G8 III–IV	P	43/23	2.52	0.07	2.66	0.08	7.4	0.2
8974.....	γ Cep	K1 III–IV	P	18/11	3.06	0.03	3.24	0.03	4.79	0.06
9045.....	ρ Cas	G2 0e	B	9/7	2.36	0.05	2.47	0.05	950	2000[b]

[a] Reference code for the spectral type, where "P" means the type is taken from Keenan & McNeil 1989, "B" from the Bright Star Catalogue (Hoffleit & Jaschek 1982), and "M" from Morgan 1972.

[b] The large uncertainty is due to a *Hipparcos* parallax of 0.28 ± 0.58 mas (Perryman et al. 1997).

limb-darkened diameter (θ_L). The ideal procedure for determining θ_L would be to fit a model atmosphere brightness distribution directly to the observed V^2 as a function of wavelength. This has the disadvantage of inserting an untested model dependence into the derived quantity. Instead, we have adopted two simplifications in the conversion of θ_U to θ_L. The first simplification is to assume a single conversion factor from θ_U to θ_L that corresponds to our mean wavelength of 740 nm (rather than convert diameters at each wavelength). This method uses an average correction factor appropriate to the temperature and surface gravity of the star, estimated from its spectral type. We multiplied the mean θ_U by this average correction factor to obtain θ_L. The multiplicative limb-darkening correction

factor used is an average of the R- and I-band quadratic limb-darkening coefficients computed by Claret, Díaz-Cordovés, & Giménez (1995). This corresponds to a wavelength of approximately 790 nm, compared with our 740 nm mean wavelength. An alternative approach would have been to compute the correction factor at 740 nm by linear interpolation. This approach yields a change of the correction factor of less than 0.5% over the range of spectral types from A0 to M0 among the luminosity class III stars.

The second simplification is that we chose the single scaling factor to correspond to a measurement having $V^2 = 0.25$, similar to the technique adopted by Mozurkewich et al. (1999) for the Mark III observations, where $V^2 = 0.3$ was used. Because our estimated diameters are not all made from observations having $V^2 = 0.25$, there will be a systematic error introduced by this simplification. From model calculations, we estimate that no more than a 0.5% error in the computed limb-darkened diameter results from this assumption, over the range of visibilities $0.1 \leq V^2 \leq 0.8$. In calculating the error in θ_L, this error of 0.5% has been added in quadrature to the scaled error of θ_U.

In order to apply the limb-darkening correction factor, we need to know the effective temperature of the star in question. We used the relationship between spectral classification, effective temperature, and surface gravity tabulated by Straižys & Kuriliene (1981) to develop a table of limb-darkening corrections as a function of spectral type for each luminosity class. Then, with the known spectral classification of the stars in our program, we were able to select the appropriate limb-darkening correction factor. Note, however, that the limb-darkening correction factors are only weakly dependent upon the temperature and gravity. For example, a change of spectral type from F0 to G0 produces a variation of less than 1% in the correction factor, while a change from K0 to M0 produces a variation of slightly more than 1%, for the range of luminosities found in our stars. Thus, the limb-darkened diameters can safely be used in a subsequent analysis to refine the effective temperature of these stars.

Once we determined θ_L for each star, we used the *Hipparcos*-derived parallaxes (Perryman et al. 1997) to calculate linear radii for the stars in the sample. Table 2 presents the diameters for the 50 stars in this paper, where the columns are as follows: (1) HR number, (2) name, (3) spectral type, (4) spectral type reference, (5) number of scans/number of independent scans, (6) uniform-disk diameter, (7) uniform-disk diameter uncertainty, (8) limb-darkened disk diameter, (9) limb-darkened disk diameter uncertainty, (10) linear radius, (11) linear radius uncertainty.

6. COMPARISON WITH OTHER DIAMETER ESTIMATES

The largest body of observational data that overlaps with our sample of stars is the set of diameters measured with the Mark III interferometer (Mozurkewich et al. 1999). These observations were made in four wavelength bands, with the most data obtained at 800 nm, close to our mean wavelength of 740 nm. The 14 stellar diameters measured in common are shown as circles in Figure 6, where we have plotted the difference between the NPOI and the Mark III θ_U as a function of the NPOI diameter. Note that Mozurkewich et al. also used quadratic limb-darkening coefficients to obtain limb-darkening corrections, so the difference between our two sets of θ_L will be in the same sense as for the θ_U. For the group of stars measured in common, the Mark III diameters average 0.07 ± 0.08 mas larger than the NPOI diameters for the entire sample. Averaging the percent differences for the entire set, we obtain an offset of $2.2\% \pm 2.5\%$. We have looked into several effects that may account for this slight difference, including incompletely corrected noise bias in V^2, systematic departures from the expected diameter based upon the color and brightness of the star (see Hutter et al. 1989), and incorrect estimates of calibrator diameters. At present, we have no explanation for the systematic difference in the diameters as obtained by these two instruments. We are currently engaged in a program to observe more stars with Mark III diameters in an effort to make a large-scale comparison between the two interferometers.

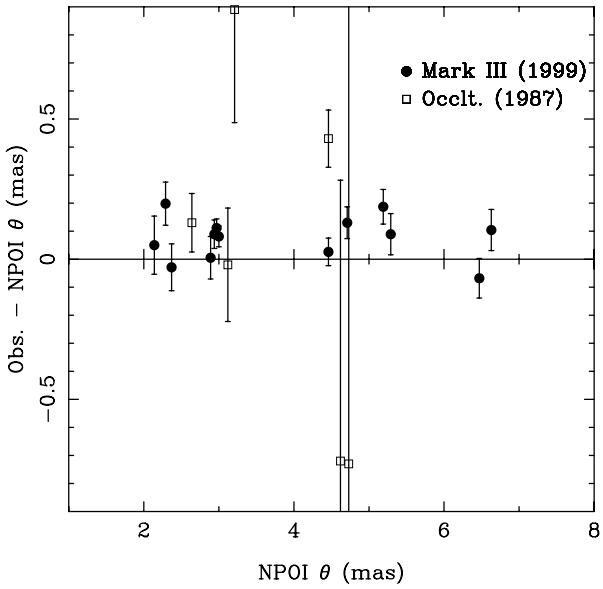

FIG. 6.—Comparison of the NPOI angular diameters with those measured by the Mark III interferometer (Mozurkewich et al. 1999) and with those measured by lunar occultations (White & Feierman 1987). The filled and open symbols are comparisons with Mark III and lunar occultation data, respectively.

In addition, although PTI is observing stars of comparable angular size (van Belle et al. 1999), there are no stars in common between our two surveys. The percent diameter errors being quoted by both groups are, however, of similar size.

We also compared our results with lunar occultation observations. We have five stars in common with the target list of White & Feierman (1987). The comparison here is not quite so straightforward, since the lunar occultation data have been made over a range of wavelengths and some have θ_U while others give only θ_L. Also, the lunar occultation errors are generally much larger than ours. We chose the closest wavelengths available in the White & Feierman catalog and compared θ_U or θ_L where appropriate. These are shown as the squares plotted in Figure 6. For the overlapping sample the rms difference is -0.01 ± 0.60 mas, and so we claim no significant difference.

Hajian et al. (1998) have used linear coefficients tabulated by Van Hamme (1993) to obtain limb-darkened diameters for α Ari and α Cas with the NPOI. They also used the triple amplitudes to derive a mean diameter and used a larger

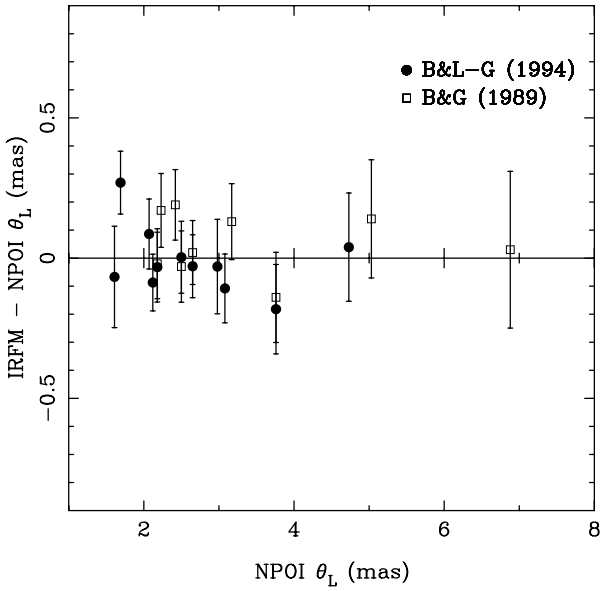

FIG. 7.—Comparison of θ_L obtained at NPOI with diameter estimates using the IRFM. The filled and open symbols correspond to comparisons with Blackwell & Lynas-Gray (1994) and Bell & Gustafsson (1989), respectively.

spectral range (20 channels) in order to emphasize the effects of limb darkening. We have rereduced these data using quadratic limb-darkening coefficients from Claret et al. (1995) and only the 10 reddest spectral channels. Our results for the limb-darkened diameter for α Ari and α Cas are 6.88 ± 0.04 and 5.60 ± 0.06 mas, respectively, while Hajian et al. obtained 6.80 ± 0.07 and 5.62 ± 0.06 mas. We have extended this comparison to several other stars in the data set and generally find that, when identical scan data sets are used, the two reduction schemes produce diameters that differ by less than about 0.02 mas with no apparent systematic difference. We believe these comparisons demonstrate the robust nature of the reduction schemes and justify our decision to scale the θ_U rather than to fit the observed V^2.

Finally, we may compare our limb-darkened diameters to those estimated using the infrared flux method (IRFM) by Bell & Gustafsson (1989) and Blackwell & Lynas-Gray (1994). From those two papers, there are 20 stars in common with our measurements. Figure 7 shows a comparison between the computed and measured diameters in this sample, where the mean difference is only 0.02 ± 0.12 mas (0.7% for a diameter of 3 mas).

7. CONCLUSIONS

We have demonstrated that the NPOI is capable of repeatable measurements of stellar angular diameters larger than about 3 mas with a precision of 1%; for smaller diameters, the errors are larger. A comparison of NPOI results with those from the Mark III indicates a systematic difference of $2.2\% \pm 2.5\%$ for all stars measured in common. A comparison of our simplified means to obtain θ_L with the approach used by Hajian et al. yielded differences in diameters of order 1%. In addition, a comparison of θ_L obtained from our measurements and angular diameters determined by the IRFM also indicates a difference of about 1%. These last two statements suggest that the agreement between model atmosphere theory and observation is on the order of 1%.

We are also making progress toward the measurement of smaller angular diameters. For example, we report a number of stars in this program with $\theta_U < 3$ mas. When there are repeated observations, the level of precision is found to be in the range 5%–7%; here the limit is set by the measurement errors for the longest baseline presently in operation. With the addition of longer baselines at the NPOI in the near future, we anticipate that the errors in these smaller diameter stars will become comparable to those observed for the larger stars in the present program. With longer baselines and with efforts to reduce the effects of atmospheric turbulence, we will obtain greater accuracy in the measurement of angular diameters, and we may be able to resolve the issue of the systematic difference between the Mark III and NPOI observations.

This research was funded by the Office of Naval Research and the Oceanographer of the Navy. We would like to thank Ben Burress, Craig Denison, and Cathy Sachs for able operation of the facility during the collection of the data, and Bob Calder, Karl Isbrecht, and James Howard for helping to keep the facility running smoothly. Jim Clark, Long Ha, and the USNO instrument shop have provided timely improvements and upgrades to the interferometer during this project. We have used the SIMBAD database, operated at CDS, Strasbourg, France, for this research.

REFERENCES

Armstrong, J. T., et al. 1998, ApJ, 496, 550
Bell, R. A., & Gustafsson, B. 1989, MNRAS, 236, 653
Benson, J. A., et al. 1997, AJ, 114, 1221
Blackwell, D. E., & Lynas-Gray, A. E. 1994, A&A, 282, 899
Claret, A., Díaz-Cordovés, J., & Giménez, A. 1995, A&AS, 114, 247
Davis, J., & Tango, W. J. 1996, PASP, 108, 456
Hajian, A. R., et al. 1998, ApJ, 496, 484
Hoffleit, D., & Jaschek, C. 1982, The Bright Star Catalogue (4th rev. ed.; New Haven: Yale Univ. Obs.)
Hummel, C. A., Mozurkewich, D., Armstrong, J. T., Hajian, A. R., Elias, N. M., II, & Hutter, D. J. 1998, AJ, 116, 2536
Hutter, D. J., et al. 1989, ApJ, 340, 1103
Keenan, P. C., & McNeil, R. C. 1989, ApJS, 71, 245
Morgan, W. W. 1972, AJ, 77, 35
Mozurkewich, D., et al. 1999, in preparation
———. 1991, AJ, 101, 2207
Perryman, M. A. C., et al. 1997, A&A, 323, L49
Straižys, V., & Kuriliene, G. 1981, Ap&SS, 80, 353
van Belle, G. T., et al. 1999, AJ, 117, 521
Van Hamme, W. 1993, AJ, 106, 2096
White, N. M., & Feierman, B. H. 1987, AJ, 94, 751